Journal of Applied Polymer Science

Fabrication, Characterization, and Properties of Poly(ethylene-co-vinyl acetate)/Magnetite Nanocomposites

M. T. Ramesan
Department of Chemistry, University of Calicut, Kerala 673 635, India
Correspondence to: M. T. Ramesan (E-mail: mtramesan@hotmail.com)

ABSTRACT: Poly(ethylene-co-vinyl acetate) (EVA)/magnetite (Fe_3O_4) nanocomposite was prepared with different loading of Fe_3O_4 nanoparticles. The mixing and compounding were carried out on a two-roll mixing mill and the sheets were prepared in a compression-molding machine. The effect of loading of nanoparticles in EVA was investigated thoroughly by different characterization technique such as transmission electron microscopy (TEM), X-ray diffraction (XRD), differential scanning calorimetry (DSC), thermogravimetric analysis (TGA), limiting oxygen index (LOI), and technological properties. TEM analysis showed the uniform dispersion of filler in the polymer matrix and the dispersion of filler decreased with increase in filler content. XRD of the nanocomposite revealed the more ordered structure of the polymer chain. An appreciable increase in glass transition temperature was observed owing to the restricted mobility of Fe_3O_4-filled EVA nanocomposite. TGA and flame resistance studies indicated that the composites attain better thermal and flame resistance than EVA owing to the interaction of filler and polymer segments. Mechanical properties such as tensile strength, tear resistance, and modulus were increased for composites up to 7 phr of filler, which is presumably owing to aggregation of Fe_3O_4 nanoparticle at higher loading. The presence of Fe_3O_4 nanoparticles in the polymer matrix reduced the elongation at break and impact strength while improved hardness of the composite than unfilled EVA. The change in technological properties had been correlated with the variation of polymer–filler interaction estimated from the swelling behavior. © 2013 Wiley Periodicals, Inc. J. Appl. Polym. Sci. **2014**, *131*, 40116.

KEYWORDS: composites; X-ray; differential scanning calorimetry (DSC); thermogravimetric analysis (TGA); swelling

Received 16 July 2013; accepted 23 October 2013
DOI: 10.1002/app.40116

INTRODUCTION

A common practice to enhance the mechanical properties of elastomer is the introduction of chemical crosslink as well as the addition of finely divided particulates, typically carbon black and silica. A minimum of 20–40 weight percentages of conventional filler is required to attain an optimum mechanical property, but this high concentration reduces the processability and increase the weight of final product. The continuous demand for new, low-cost, and light-weight elastomer composites with improved properties represents challenge in the polymer industry. Polymer nanocomposites offer the possibility for new alternatives. The inclusion of nano-sized particles enables the enhancement of properties in polymers with even at small amount of fillers, a feature not achieved by conventional composites. It was found that the inclusion of 10 weight percentage of filler greatly improves the mechanical properties of polymer over conventionally filled system.[1–3] The physical and chemical properties of nanocomposites are different from their bulk counterparts because of the nanometer-scale dispersion of reinforcement filler and the high surface to volume ratio.[4–6]

Poly(ethylene-*co*-vinyl acetate) polymers have a large commercial impact because of their broad spectrum of practical applications in different fields. The polymer is extensively used in many engineering and industrial areas because of its toughness, and biological inertness, waterproofing, corrosion protection, and packaging of components.[7,8] Ethylene/vinyl acetate copolymers with different vinyl acetate are available as rubbers, thermoplastic elastomers, and plastics, which in turn provide this broad spectrum of uses. Because of the high extent of commercial importance, recently researchers have made an intense focus on ethylene vinyl acetate (EVA) composites filled with different metal nanoparticles.[9,10] Various research groups focused on EVA/clay nanocomposites because of its amazing improvements in mechanical properties, thermal resistance, reduced gas permeability, and flame retardancy when compared with pure EVA and its conventional polymer composite.[11–13] It is well known that these properties depend on different factors such as size and shape of nanoparticles, crystallinity, polarity, and degree of dispersion of filler in the polymer.

The vast majority of the work in polymer nanocomposite has been focused on the use of montmorillonite-type clays as

nanoparticles. However, iron oxide nanoparticles especially magnetite (Fe_3O_4) have been of scientific and technological interest in the last few decades.[14–16] The traditional ceramic magnetic materials are replaced by magnetic elastomer because of their mold ability, low cost, and light weight. They are also promising characteristics such as high saturation magnetic induction, low coercivity, high permeability, and low high-frequency loss, which can be widely used in microwave absorbers, sensors, automobile, petroleum, and chemical industries.[17] The iron oxide nanoparticles exhibit different oxidation states of iron, which determines their specific properties in composites. The combination of elastic and magnetic properties has opened up new possibilities for different technological applications such as magnetorheological elastomers and thermal- and flame-resistant magnetoelastic composite with variable conductivity and magnetic properties. This work focused on a simple, inexpensive, and environmentally friendly Fe_3O_4 nanoparticle-incorporated EVA copolymer. The morphology of the composite and the dispersion of filler in the polymer matrix were investigated using transmission electron microscopy (TEM) and X-ray diffraction (XRD). The thermal behaviors, flammability, swelling characteristics, and mechanical properties of the composites were also evaluated.

EXPERIMENTAL

Materials

Poly(ethylene-*co*-vinyl acetate) was supplied by Polyolefin Industries Limited, Chennai, India. The vinyl acetate content was 18%. The additives such as zinc oxide (ZnO) and dicumyl peroxide (DCP) used were of commercial grade. Toluene, ferrous chloride tetrahydrate ($FeCl_2{\cdot}4H_2O$), and iron trichloride ($FeCl_3$) were obtained from Nice India Chemicals.

Preparation of Fe_3O_4 Nanoparticles

The preparation of nano-Fe_3O_4 particles (32-nm size) was performed by a chemical coprecipitation technique described previously.[16] About 8.0 g of $FeCl_3{\cdot}H_2O$ and 3.60 g of $FeCl_2{\cdot}4H_2O$ were dissolved in 150 mL of deionized water in a 500-mL four-necked Erlenmeyer flask equipped with a condenser, a nitrogen inlet, and a mechanical stirrer. The mixture was stirred under N_2 for 30 min, followed by rapid addition of 80 mL 15*M* ammonia into the solution to regulate pH up to 11. The reaction was allowed to proceed at 50°C for 6 h. The reaction mixture was cooled in an ice bath and centrifuged at 3000 rpm to collect a black precipitate. After the precipitate was rinsed by deionized water to remove excess ions until neutrality, ethanol was used to syringe the sample thrice and dried at 40°C for 24 h, yielding Fe_3O_4 nanoparticles.

Preparation of EVA/Fe_3O_4 Nanocomposites

The mixing of EVA with various ingredients was carried out on a two-roll mixing mill (150 mm × 300 mm) with a friction ratio 1 : 1.4 as per ASTM D 15–627. The EVA granules were sheeted out first and then mixed with 4 phr of ZnO. The amount of curing agent, DCP, was kept constant (5 phr) for all the mixes. Special attention was taken to attain uniform distribution of nanoparticles. The magnetic nanocomposites based on EVA have been processed with Fe_3O_4 ratios varying from 0, 3, 5, 7, and 10 phr.

Cure Characteristics

The cure characteristics were studied by means of an oscillating disc rheometer (Monsanto Rheometer MDR-2000, USA) as per ASTM standard D 5289 (2001). The samples were vulcanized at 160°C using a hydraulic press, having electrically heated platens, under a pressure of 689.4 kPa (mold dimension: 150 mm × 150 mm × 2 mm) to their respective vulcanization time.

X-Ray Diffraction Analysis

An XRD measurement was recorded using Philips X-ray diffractometer using CuK_α radiation ($\lambda = 1.5406$ Å) running at 40 kV and 40 mA so as to acquire information of the crystal structure of the samples. The diffractogram was recorded in terms of 2θ in the range of 5°–80°. The operating voltage and the current of the tube were kept same throughout the investigation.

Transmission Electron Microscopy

Transmission electron micrographs of the samples were taken using a Philips CM12 model with an acceleration voltage of 100 kV. The specimens were prepared using an Ultracut E cryomicrotome. Thin sections of about 100 nm were cut with a diamond knife at −100°C.

Differential Scanning Calorimetry

The changes in glass transition temperature of the composites were noticed using Perkin–Elmer differential scanning calorimetry (DSC) thermal analyzer. For the DSC analysis about 5 mg of the samples was heated from −40 to 150°C under nitrogen atmosphere with a programmed heating rate of 10°C/min.

Thermal Degradation Studies

Thermal stability of EVA and its hybrids was investigated using Perkin–Elmer Thermal Analyzer. TGA and DTG measurements were carried out between ambient temperature and 600°C at a heating rate of 20°C/min in nitrogen gas purge.

Testing of Rubber Vulcanizate

The tensile strength and tear resistance of the compounds were carried out using a Zwick Universal Testing Machine (UTM) at 28°C and at a crosshead speed of 500 mm/min according to ASTM D 412-80 and ASTM D 624-81, respectively. Hardness of the samples was measured according to ASTM D 2240-81 using a Shore A-type durometer. Izod impact strength of the vulcanized samples was performed in an Instrumented Impact tester (model Resil Impactor) with 2 J capacity using notched specimens. The tests were conducted at room temperature according to ASTM D 256 method.

Limiting Oxygen Index

The flame retardancy test of the vulcanizate was carried out by limiting oxygen index (LOI) test as per ASTM D 2863-97 procedure. The vulcanized sample was burned in a Stanton Redcroft FTA flammability unit under nitrogen–oxygen environment. The minimum concentration of the oxygen in the oxygen–nitrogen gas environment just sufficient to sustain the flame for 30 s was used for calculating LOI values using the formula:

$$\text{LOI} = \text{volume of oxygen} / (\text{volume of nitrogen} + \text{volume of oxygen}) \times 100 \quad (1)$$

Polymer–Filler Interaction

Polymer–filler interaction was used to study the reinforcement of filler in the polymer matrix. Samples with dimension of 50

Table I. Cure Characteristics of Magnetite Nanoparticles-Incorporated EVA

Samples	Cure time (min)	Max. torque (dNm)	Min. torque (dNm)
EVA	15	17	1.8
EVA/3 phr Fe_3O_4	14	19	1.9
EVA/5 phr Fe_3O_4	12.75	22	2.1
EVA/7 phr Fe_3O_4	11.25	25.7	2.2
EVA/10 phr Fe_3O_4	10	25.5	2.2

mm × 30 mm × 2 mm were immersed in toluene at room temperature until equilibrium swelling. The swollen sample was weighed and the solvent is removed by drying and weighed again. The volume fraction of EVA in the swollen vulcanizate (V_r) was calculated using the following equation

$$V_r = \frac{(d-f_w)\rho_r - 1}{(d-f_w)\rho_r - 1 + A_s\rho_s - 1},$$

where A_s is the amount of solvent absorbed, ρ_r and ρ_s are the density of polymer and solvent, respectively, d is the deswollen weight of the sample, and f_w is the fraction of insoluble components. Density of the samples was determined by Electronic Densimeter HD-200 S. The densities of EVA with 0, 3, 5, 7, and 10 phr of Fe_3O_4 are 0.96, 0.99, 1.08, 1.17, and 1.28 g/cm^3, respectively.

RESULTS AND DISCUSSION

Cure Characteristics

Cure characteristics are determined from the corresponding curing isotherms at 160°C. Influence of Fe_3O_4 on the cure characteristics of EVA with different concentration of nanoparticle is shown in Table I. The optimum cure time of EVA/Fe_3O_4 composite decreases with the increase in concentration of Fe_3O_4 particles. In comparison with unfilled sample, the addition of Fe_3O_4 caused the reduction of cure time from about 15 to ~10 min (for the composite with 10 phr of Fe_3O_4 particles). This trend is similar to those found in magnetic rubber composites that confirm the effect of fillers on chain crosslink process.[18] In addition, certain metals have the catalytic effect on the cure reaction.[19] The reduction in optimum cure time may possibly due to the increased thermal conductivity of the composite system, resulting from the formation of conductive chains between the filler and polymer.[20] Minimum torque is the shear force acting on the composite before the complete vulcanization and it is related to viscosity. Viscosity of the polymer composite depends on mixing and the type of filler. In this study, each polymer mixing takes relatively short time, so the dominant factors that influence the viscosity are the size and shape of filler. Minimum torque increases with an increase in the content of Fe_3O_4 nanoparticles owing to the reinforcing nature of the filler in the matrix. The polar groups present in both polymer and filler brought together by the mechanical mixing lead to the chemical interaction between them. Also, the shear force developed during the mechanical mixing of polymer with filler makes the nanoparticles alignment in a uniform way. Maximum torque is the value that occurs after the complete vulcanization of polymers and it is the measure of modulus and crosslink density. Maximum torque increases gradually as dosage of Fe_3O_4 in EVA increases up to 7 phr. The increase in rheometric torque is attributed to the better polymer–filler interaction that becomes more pronounced in 7 phr of filler loading. It is already reported that maximum torque is dependent on the crosslink density and chain entanglements. At higher loading (10 phr), the magnetic filler reduces the macromolecular chain entanglements and thus level off the minimum torque value.

Transmission Electron Microscopy

The surface morphology of EVA/Fe_3O_4 nanocomposite with different concentration of nanoparticles is given in Figure 1. TEM images of composite with lower concentration of Fe_3O_4 show an irregular structure with globular particles that is due to poor chemical interaction between the filler and polymer. As the concentration of nanoparticles increased to 7 phr, the nanoparticles are well dispersed in EVA with spherically shaped particle having very good uniformity and adhesiveness. Generally, nano-sized particles have large surface area while the polymer containing polar group has high affinity to iron oxide leading to orientation of nanoparticles inside the macromolecular chain of EVA. The more ordered structure of polymer composite is due to the coordination interaction between empty orbit of the iron atom in Fe_3O_4 nanoparticles and the oxygen atom of vinyl acetate segment of EVA. When the concentration of Fe_3O_4 nanoparticles increased to 10 phr, the morphology of the composite has remarkably changed from a spherical structure into an irregular structure. Also, it can be observed that the nanoparticles became aggregated at higher loading of filler. This is because Fe_3O_4 nanoparticles cannot easily move into the macromolecular chain of EVA owing to the poor interfacial interaction between the filler and the polymer, which leads to an increase in free volume of the samples.

XRD Analysis

XRD of EVA vulcanizate [Figure 2(1)] shows a strong reflection peak at $2\theta = 20.7$ and four more weak reflection peaks at 31.5°, 34.2°, 47.3°, and 56.5°, whose *hkl* planes are110, 200, 210, 020, and 220, respectively.[21,22] Figure 2(2) reveals the XRD pattern of iron oxide that indicates the crystalline nature of Fe_3O_4 particles and the peaks obtained at $2\theta = 35.3°$, 56.9°, and 62.3° correspond to the diffraction of 311, 511, and 440 crystal plane of pure Fe_3O_4, respectively.[23] The XRD curve of nano-Fe_3O_4-incorporated copolymer vulcanizate exhibits all the characteristic peaks of EVA along with the crystalline peaks of Fe_3O_4 owing to the systematic alignment of polymer chain. It is interesting to observe that the addition of Fe_3O_4 nanoparticles to the copolymer leads to the shift of diffraction peak to a higher angle with respect to that of pure EVA [Figure 2(3 & 4)]. As the Fe_3O_4 have nano-dimension, they are inserted in between the macromolecular chains that cause the change in interlayer volume and hence the corresponding layer spacing. This increased layer spacing gives rise to the shifting of diffraction peaks to higher angles. The *d*-spacing for the composite samples containing 7 and 10 wt % of Fe_3O_4 is given in Table II. It is found that in all systems, the interlayer spacing increases owing to the increased polarity of both EVA and the filler. With the

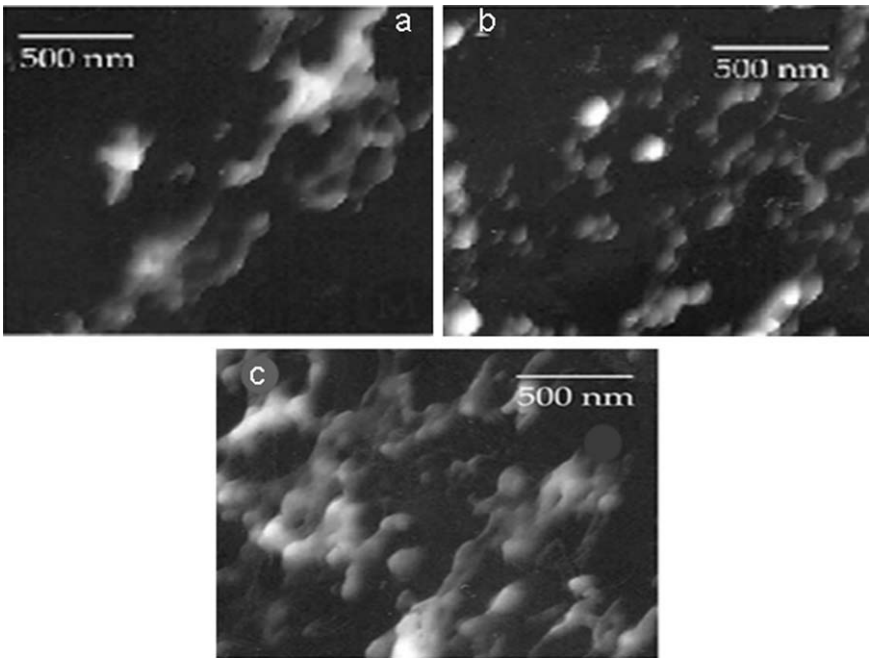

Figure 1. TEM images for the EVA with (a) 3 phr, (b) 7 phr, and (c) 10 phr magnetite nanoparticles.

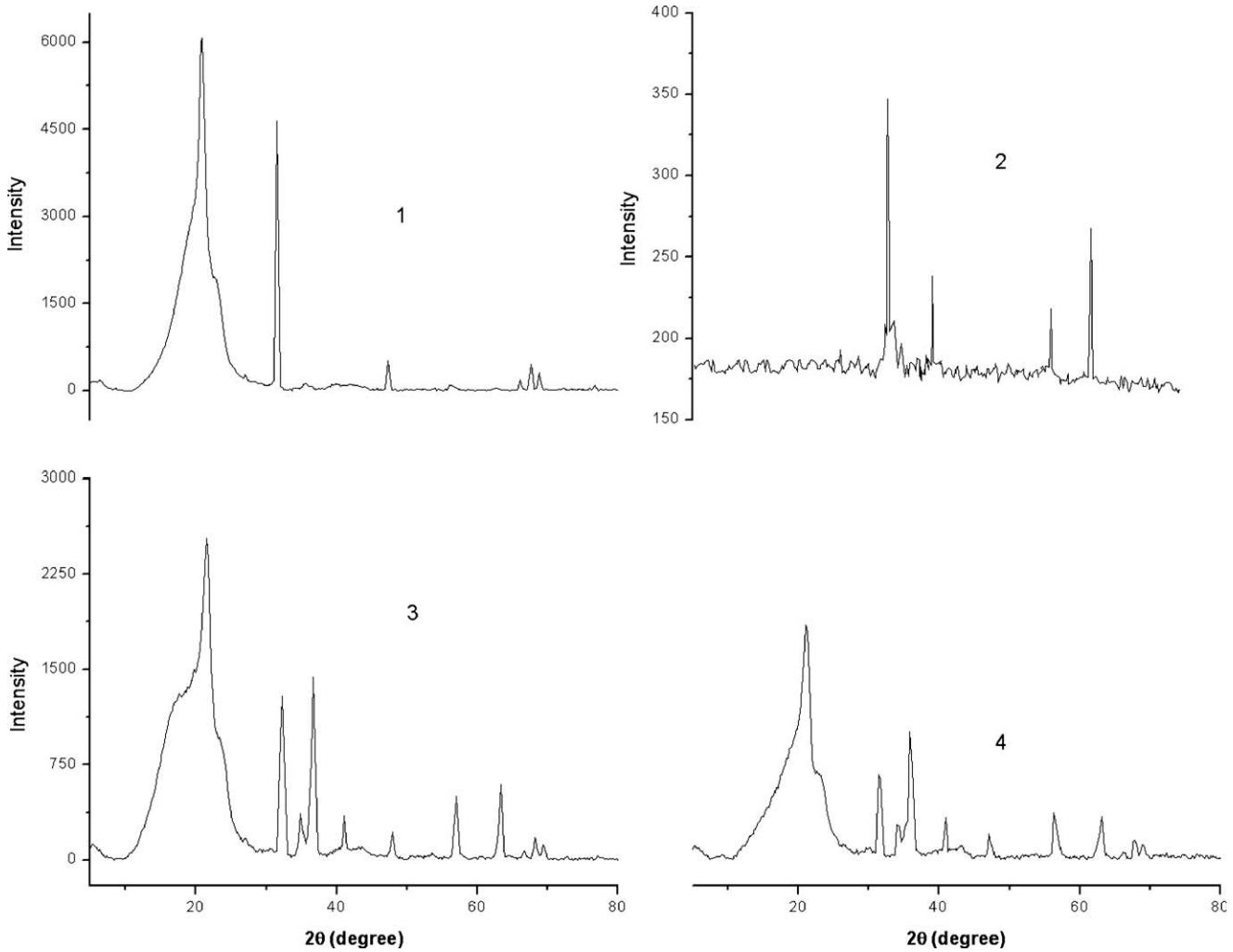

Figure 2. XRD curve of (1) EVA, (2) Fe_3O_4, (3) EVA with 7 phr, and (4) EVA with 10 phr of Fe_3O_4 nanoparticles.

Table II. *d*-Spacing and the 2θ Value of EVA and Its Nanocomposites

Samples	2θ	*d*-Spacing (Å)
EVA	20.71	4.25
	31.37	2.84
	34.06	2.62
	47.15	1.92
	56.31	1.63
EVA/7 phr Fe_3O_4	21.62	3.93
	32.3	2.77
	36.73	2.44
	41.05	2.19
	49.96	1.89
	57.06	1.61
	63.36	1.03
EVA/10 phr Fe_3O_4	21.06	4.02
	31.57	2.83
	35.95	2.51
	41.07	2.19
	47.13	1.92
	56.38	1.63
	63.06	1.47

increase of filler content, the right shift magnitude of diffraction peak decreases with respect to 7 phr of composite, that is, the enlargement in extent of interlayer distance of the Fe_3O_4 decreases. Some nanoparticles still maintain a little ordering of Fe_3O_4-layered structure, but tend to show a random dispersion of filler at higher loading. This claim is in good agreement with the TEM studies. This indicates that 7 phr of Fe_3O_4 is more favorable for the interaction of EVA chains with the nanoparticles. Hence, it can be deduced that the Fe_3O_4 nanoparticles are not simply mixed up or blended rather than they are strongly trapped inside the copolymer chain owing to the strong polar–polar interaction between the filler and EVA.

DSC Curve of EVA/Fe_3O_4

DSC measurements are useful for the identification of crystallization, melting, and the extent of interaction of nanoparticles in the matrix. DSC scan of EVA and EVA/Fe_3O_4 nanocomposites is given in Figure 3. All the samples exhibit multiple melting endotherms, which are composed of a slight endotherm started at a low temperature (glass transition temperature), a major melting peak at the end, and a weak peak between them. The endotherm at low temperature is due to the secondary crystallization behavior; while the small and major peaks represent the primary crystallization.[24,25] The glass transition temperatures (T_g) of all the polymers are below 50°C, which falls in the category of soft polymers having flexible backbone as reflected in their structure. The DSC studies of EVA showed a T_g at 29.8°C, whereas the Fe_3O_4-incorporated EVA composite showed the heat of inflection at higher temperatures with an increase of about 3.9 and 7.3°C (i.e., 33.7 and 37.1°C) for 5 and 7 phr, respectively. The segmental mobility of polymer matrix is much affected by the interaction between the polar groups of Fe_3O_4 with the vinyl acetate group of EVA and thereby enhances the glass transition temperature.

The melting temperature (T_m) and the heat of melting (ΔH_f) for all the composites are determined from DSC results (Figure 3) and the data are shown in Table III. The primary (T_{m1}) and secondary crystallization melting (T_{m2}) of the composite (5 phr Fe_3O_4/EVA) is slightly higher than that of pure EVA, whereas the value decreased with further increase in concentration of nanoparticles. This indicates that lower loading of Fe_3O_4 is sufficient for the interaction of nanoparticle with vinyl acetate leading to longer crystallizable ethylene chain segments, which is positive for spherulite growth and crystal perfection.[26]

The relative crystallinity (X_c) of the samples was calculated with the following equation:

$$X_c = \Delta H_f / \Delta H^* f \times 100(\%) \quad (2)$$

where $\Delta H^* f$ is the fusion enthalpy of the perfect polyethylene (277.1 J/g) crystal[25] and ΔH_f is the enthalpy of fusion of the EVA samples. As listed in Table III, the primary crystallization melting peak position of EVA/Fe_3O_4 keeps higher than that of pure EVA in all cases. The decrease in crystallinity of the composite (Table III) is attributed to the inclusion of rigid Fe_3O_4 particles into the vinyl acetate units of copolymer backbone.

Thermal Degradation Studies of EVA and Its Nanocomposite

The thermal behavior (TGA and DTG) of EVA and Fe_3O_4 nanoparticles-filled composites is shown in Figure 4. Thermal degradation of EVA shows two stages of weight loss, where the first stage (at 319°C) is assigned to the removal of acetic acid from the vinyl acetate group and the second stage (at 430°C) is due to the degradation of the unsaturated polyethylenic chains.[27,28] The thermal stability of nanocomposite depends upon the dispersion of nanoparticles in the polymer matrix. From the DTG curves it can be observed that the initial and final decomposition temperatures are increased with the addition of Fe_3O_4 nanoparticles, which is an indication of better

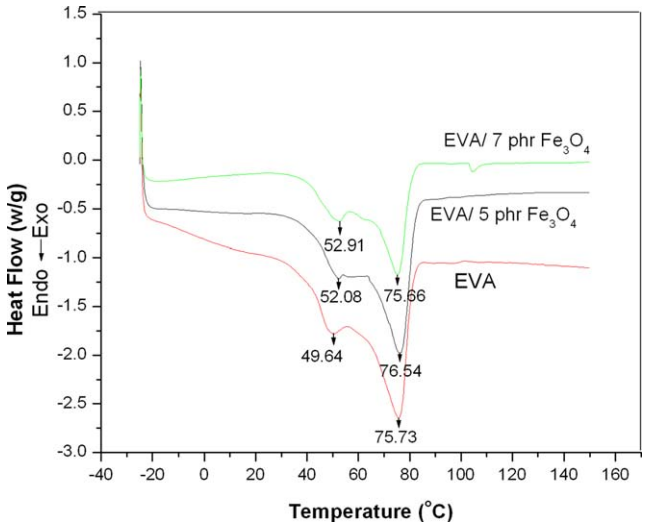

Figure 3. DSC curves of EVA and magnetite nanoparticle-filled EVA. [Color figure can be viewed in the online issue, which is available at wileyonlinelibrary.com.]

Table III. The Melting Temperature (T_m) and the Heat of Melting (ΔH_f) EVA/Fe_3O_4 Nanocomposite

Samples	T_g (°C)	T_{m1} (°C)	T_{m2} (°C)	ΔH_{f1} (J/g)	ΔH_{f2} (J/g)	X_{c1} (%)	X_{c2} (%)
EVA	29.8	49. 64	75.73	14.82	49.13	5.34	17.73
EVA/5 phr Fe3O4	33.7	52.08	76.54	2.97	26.12	1.07	9.43
EVA/7 phr Fe3O4	37.1	52.91	75.66	5.27	16.68	1.91	6.01

thermal stability of the system. For example, the initial decomposition temperature is increased by 19 and 30°C, whereas the final degradation temperature is raised by 10 and 18°C for the composite containing 7 and 10 phr of Fe_3O_4 nanoparticles, respectively. This can be explained based on the fact that the availability of surface area of the nanoparticle per unit volume increased in the matrix that leads to the formation of protective layer against the degradation of polymer.

Mechanical Properties

The effect of the Fe_3O_4 content on mechanical properties of the copolymer is summarized Table IV. The tensile strength and tear resistance of the hybrids are increased with an increase in filler content up to 7 wt % of Fe_3O_4 in EVA matrix. It is also evident from table that the tensile strength is increased by 19, 39, 61, and 57% and the tear resistance is increased by 6, 20, 32, and 30% for composites containing 3, 5, 7, and 10 wt % Fe_3O_4, respectively, in the polymer matrix. The increase in tensile and tear properties of nanocomposites indicated that EVA is strengthened and toughened simultaneously by the uniform dispersion of Fe_3O_4 nanoparticles in the matrix. The homogeneously dispersed nanoparticles in the polymer matrix (as evident from TEM images) offer the whole surface of the spin-polarized Fe_3O_4 layers for the interactions with the polymer chain. The strong interfacial interaction between the vinyl acetate unit and the Fe_3O_4 particles leads to the corresponding increase in the tensile and tear strength of nanocomposites. It can be clearly observed that the tensile and tear properties start to decrease with further increase in Fe_3O_4 content (above 7 phr) in the composite. This decrease in mechanical properties is due to the agglomeration of filler particles or simply the result of physical contact between adjacent agglomerates. The agglomerate is a domain that can behave like a foreign body in the composites; this agglomerate reduces the movement of macromolecular chain and initiate failure under stress. The effect of filler loading on elongation at break of the nanocomposite is given in Table IV. The elongation at break of the composite decreased with increasing the loading of fillers. This result demonstrates that the nanoparticles hardened the composite and reduced their ductility. The modulus at 300% elongation of EVA/Fe_3O_4 nanocomposites is given in Table IV. It shows an enhancement of modulus as the Fe_3O_4 content increases. This result is in good agreement with the previous maximum torque data obtained where the addition of filler to EVA increases the maximum torque value. The increase in modulus indicates the increase in stiffness of the nanocomposite. Fillers are known to increase the modulus of composite, provided that the modulus of the filler is higher than that of the polymer matrix. The enhanced modulus arises from the polymer–filler interactions; that can be increased when a good dispersion of the filler is possible with polymer, which is the characteristic of the nanoparticles and is dependent on polarity and semicrystalline nature of the polymer. When the Fe_3O_4 content exceeds 7 wt %, the modulus of the composite decreases, probably because of the aggregation of nanoparticles, as reflected by the data of the composite containing 10 wt % Fe_3O_4 shown in Table IV. Hardness of vulcanizates is usually expected to increase by the use of fillers.[29] The variation in hardness of Fe_3O_4-reinforced EVA is given in Table IV. The results reveal that the hardness of the vulcanizates increases progressively with increasing the filler loading. The increase in hardness is related with increasing surface area of the filled particles through a more efficient stress transfer from the polymer matrix to Fe_3O_4 nanoparticles and the increasing amount of nano-Fe_3O_4 particles in the polymer matrix.

Impact strength of EVA/Fe_3O_4 composites is given in Table IV. As the dosage of filler increases, the ability of the composites to absorb impact energy decreases. The results obtained show that impact property of the composites changed remarkably at higher content of filler (10 phr). The EVA nanocomposite with 7 phr of Fe_3O_4 content showed a reduction of ~9% in impact strength, whereas those prepared with 10 phr filler content shows ~18% decrease in impact strength. This decrease of deformational energy is due to the reduction in mobility of polymer chain. It is noticed that this decreasing trend is minimum up to 7 phr of filler, which is due to the strong interaction between the polymer phase and the filler particles. However, at higher loading, the

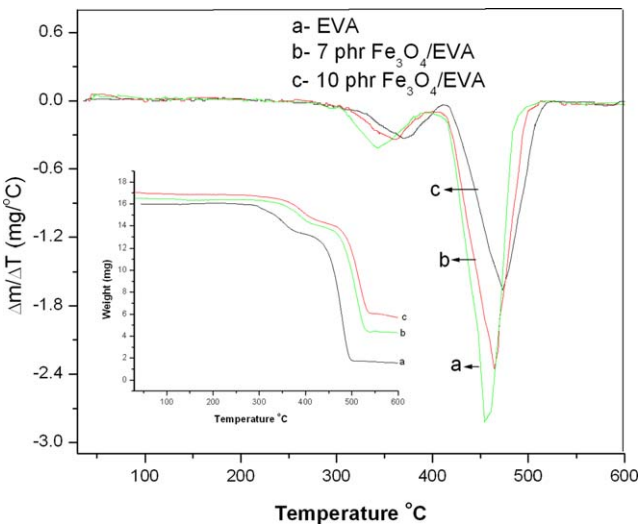

Figure 4. TGA and DTG curves of EVA and EVA/Fe_3O_4 nanocomposites. [Color figure can be viewed in the online issue, which is available at wileyonlinelibrary.com.]

Table IV. Mechanical Properties of Various Loading of Fe_3O_4-Filled EVA

Samples	Tensile strength (MPa)	Modulus at 300%	Elongation at break (%)	Tear strength (N/mm)	Hardness shore A	Impact strength (J/m)
EVA	16.14	10.24	379.6	3.85	48	164.6
EVA/3 phr Fe3O4	19.22	12.53	373.98	4.08	49	159.8
EVA/5 phr Fe3O4	22.41	14.99	366.02	4.65	50	155.5
EVA/7 phr Fe3O4	26.02	16.76	358.41	5.11	51	150.1
EVA/10 phr Fe3O4	25.44	15.21	347.78	5.02	53	134.5

nanoparticles act as a discontinuity in the polymer matrix that leads to a decrease in material homogeneity, hence weakening the material and leading to poor stress transfer between polymer matrix and the nanoparticles.[30] Thus, it can be concluded that the nanoparticles acted as stress concentrators and decreased the impact strength of the composites.

Polymer–Filler Interaction

Polymer–filler interaction is carried out by measuring the volume fraction of polymer in the swollen vulcanizate as an index of crosslink density. The extent of polymer–filler interaction (V_r) of EVA/Fe_3O_4 nanocomposite with various loading of filler is given in Figure 5. The higher the V_r, the higher will be the polymer–filler interaction. The addition of Fe_3O_4 nanoparticles inside the EVA matrix reduced the penetration of the solvent molecule into the EVA/Fe_3O_4 composite. Hence, the extent of polymer–filler interaction is higher in polymer nanocomposite when compared with EVA and the maximum polymer–filler interaction is noted up to 7 phr of Fe_3O_4 and thereafter the value decreases. The interaction between Fe_3O_4 nanoparticles and the polymer chain facilitates stress transfer to the reinforcement phase, resulting in a higher polymer–filler interaction values. These findings are in good agreement with the results obtained from tensile and tear strength studies. The poor interaction between filler and EVA at higher loading (10 phr) leads to the formation of loosely bound aggregates in the polymer matrix, which acted as a stress raisers and this provided easy path for breaking the macromolecular chain and thereby causing a decrease in V_r values.

Limiting Oxygen Index

The LOI is the direct measure of the flame resistance of material and expressed as the percentage of oxygen required for self-sustained combustion of any material. The LOI values of various loading of Fe_3O_4-filled EVA copolymer are given in Figure 5. It is clear that flame resistance of the nanocomposite is higher than that of pure EVA and the value increases with the increase in concentration of Fe_3O_4 nanoparticles. Thus, pure EVA has a LOI index of 19, whereas the nanocomposite with 10 phr of filler exhibits a LOI index of 24. The enhanced interfacial interaction between Fe_3O_4 and polymer matrix may improve the flame retardancy of composites by the improved dispersion level and heat-flow resistance. Thus, dispersion of Fe_3O_4 nanoparticles in the polymer matrix is an important criterion for obtaining better flame-retardant performance. The metal oxide nanoparticles present in the filler reduce the carbonization of the polymer forming more effective char layer. This indicates that the nanoparticle could act effectively as thermal barrier, which protects the polymer underneath the char layer. At higher loading of filler, the thickness of char layer increases, which in turn to prevent the burning of the resulting polymer. Materials with LOI value above 20.8 are classified as relatively safe, whereas substances with LOI less than 20.8, which continue to burn in oxygen-deficient air, are not safe as building material.[31] The fabricated nanocomposites exhibit better flame resistance than pure EVA and hence this composite is considered as safe for indoor applications.

CONCLUSIONS

Nanocomposite of EVA with different loading of Fe_3O_4 was prepared in a two-roll mixing mill and the cure behavior of the composite was studied. The cure time of EVA compounds decreased with the increase in filler loading but showed enhancement in minimum torque and maximum torque. The morphology of the nanocomposite was investigated using TEM. TEM image established that the nanoparticles were well dispersed in the polymer matrix (7 phr of Fe_3O_4) and the dispersion of filler decreased with an increase in the concentration of filler. The crystalline nature of the composite was studied using XRD patterns. It has been found that the diffraction peaks were shifted to higher angles along with the change in position of *d*-spacing and the shift in diffraction peak is the maximum for composite with 7 phr of nanoparticles. DSC analysis showed that the interaction

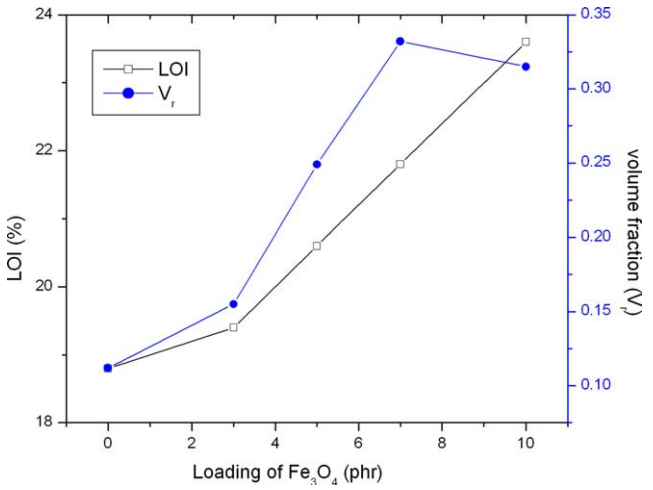

Figure 5. Flame resistance and polymer–filler interaction of EVA/Fe_3O_4 nanocomposites. [Color figure can be viewed in the online issue, which is available at wileyonlinelibrary.com.]

of Fe_3O_4 nanoparticles affected the glass transition temperature (T_g) of the soft segment of EVA. Therefore, the T_g of nanocomposite was increased with an increase in the concentration of nanoparticles. The thermal stability of the nanocomposites was significantly improved by the addition of Fe_3O_4 nanoparticles. This might have resulted from the polar–polar interaction between filler and EVA, which could be explained by the restrictions on the mobility of macromolecular chain imposed by the nanoparticles. Mechanical properties such as tensile, tear, modulus, and hardness of the composite increased with an increase in filler loading. In general, the composites containing 7 phr of Fe_3O_4 content showed better performance in tensile, tear, and modulus properties. From the impact test results, it was seen that the impact strength was affected by the nanoparticles content. The composites containing 7 phr of Fe_3O_4 showed a reduction of ~9% and the composites with 10 phr filler showed 18% of decrease in impact strength. The volume fraction of the cured nanocomposite increased with an increase in concentration of iron oxide particles up to 7 phr and thereafter the value decreased. The composite showed excellent flame retardancy than EVA and also the flame resistance of the samples increased with an increase in concentration of nanoparticles.

REFERENCES

1. Jeon, H. U.; Lee, D. H.; Choi, D. J.; Kim, M. S.; Kim, J. H.; Jeong, H. M. *J. Macromol. Sci. Part B* **2007**, *46, 1151.*
2. Arroyo, M.; Lopez-Manchado, M. A.; Herrero, B. *Polymer* **2003**, *44*, 2447.
3. Feldman, D. *J. Macromol. Sci. Part A* **2013**, *50*, 441.
4. Pinnavaia, T. J.; Beall, G. W. Polymer-Clay Nanocomposites; Wiley: New York, **2001**; Vol. *1*, Chapter 1, p 3.
5. Park, K. W.; Kim, G. H. *J. Appl. Polym. Sci.* **2009**, *112*, 1845.
6. Khan, A. S.; Wong, F. S. L.; McKay, I. J.; Whiley, R. A.; Rehman, I. U. *J. Appl. Polym. Sci.* **2013**, *127*, 439.
7. Dlamini, D. S.; Mishra, A. K.; Mamba, B. B. *J. Appl. Polym. Sci.* **2012**, *124*, 4978.
8. Zou, H.; Ma, Q.; Tian, Y.; Wu, S.; Shen, J. *Polym. Compos.* **2006**, *27*, 529.
9. Jin, B.; Zhang, W.; Sun, G.; Gu, H. B. *J. Ceramic Process. Res.* **2007**, *8*, 336.
10. Lv, J. P.; Liu, W. *J. Appl. Polym. Sci.* **2007**, *105*, 333.
11. Alexandre, M.; Beyer, G.; Henrist, C.; Cloots, R.; Rulmont, A.; Jerom, R.; Dubois, P. *Chem. Mater.* **2001**, *13*, 3830.
12. Zanetti, M.; Camino, G.; Thomann, R.; Mulhaupt, R. *Polymer* **2001**, *42*, 4501.
13. Acharya, H.; Srivastava, S. K.; Bhowmick, A. K. *Polym. Eng. Sci.* **2006**, *46*, 837.
14. Pyun, J. *Polym. Rev.* **2007**, *47*, 231.
15. Gu, Z.; Li, C.; Wang, G.; Zhang, L.; Li, X.; Wang, W.; Jin, S. *J. Polym. Sci. Part B: Polym. Phys.* **2010**, *48*, 1329.
16. Ramesan, M. T. *Int. J. Polym. Mater. Polym. Biomater.* **2013**, *62*, 277.
17. Yaghmour, S. J.; Hafez, M.; Ali, K.; Elshirbeeny, W. *Polym. Compos.* **2012**, *33*, 1672.
18. Malini, K. A.; Kurian, P.; Anantharaman, M. R. *Mater. Lett.* **2003**, *57*, 3381.
19. Sasikumar, K.; Suresh, G.; Thomas, K. A.; John, R.; Natarajan, V.; Mukundan, T.; Vishnubhatla, R. M. R. *Bull. Mater. Sci.* **2006**, *29*, 637.
20. Ramesan, M. T.; Premalatha, C. K.; Alex, R. *Plast. Rubber Compos.* **2001**, *30*, 355.
21. Kader, F. H. A.; Said, G.; Attia, G.; Fadl, A. M. A. *Egypt. J. Phys.* **2006**, *37*, 111.
22. Schwartz, K. W.; Condreck, R. B. *Adv. X-Ray Anal.* **1997**, *39*, 515.
23. Jana, N. R.; Chen, Y. F.; Peng, X. *Chem. Mater.* **2004**, *16*, 3931.
24. Yang, H.; Jiang, W.; Lu, Y. *Mater. Lett.* **2007**, *61*, 2789.
25. Shi, X. M.; Zhang, J.; Li, D. R.; Chen, S. J. *J. Appl. Polym. Sci.* **2009**, *112*, 2358.
26. Ramesan, M. T.; Lee, D. S. *Iran. Polym. J.* **2008**, *17*, 281.
27. Lee, K. Y.; Kim, K. Y. *Polym. Degrad. Stab.* **2008**, *93*, 1290.
28. Jeon, C. H.; Ryu, S. H.; Chang, Y. W. *Polym. Int.* **2003**, *52*, 153.
29. Sareena, C.; Ramesan, M. T.; Purushothaman, E. *J. Appl. Polym. Sci.* **2012**, *125*, 2322.
30. Sombatsompop, N.; Chaochanchaikul, K. *Polym. Int.* **2004**, *53*, 1210.
31. Ramesan, M. T. *J. Polym. Res.* **2004**, *11*, 333.